Electronic Supplementary Information

Synthesis of hierarchical TiO_2 nanoflower with anatase-rutile heterojunction as Ag support for efficient visible-light photocatalytic activity

Juan Zhou,[a] Guohui Tian,*[a,b] Yajie Chen,[a] Jian-Qiang Wang,[c] Xinrui Cao,[a] Yunhan Shi,[a] Kai Pan,[a] and Honggang Fu*[a]

[a] *Key Laboratory of Functional Inorganic Material Chemistry, Ministry of Education of the People's Republic of China, Heilongjiang University, Harbin 150080 P. R. China*

[b] *Key Laboratory of Chemical Engineering Process & Technology for High-efficiency Conversion, College of Heilongjiang Province, School of Chemistry and Materials Science, Heilongjiang University, Harbin 150080, China.*

[c] *Shanghai Synchrotron Radiation Facility (SSRF), Shanghai Institute of Applied Physics, Chinese Academy of Sciences, Shanghai, 201204, P. R. China.*

Corresponding author E-mail: tiangh@hlju.edu.cn; fuhg@vip.sina.com, Tel.: +86 451 8660 4330, Fax: +86 451 8667 3647

Table S1. Physicochemical properties of obtained different TiO_2 samples.

Samples	Anatase (%)	Rutile (%)	S_{BET} (m^2/g)	Pore volume (cm^3/g)	Pore size (nm)	Crystallite size (nm)	Optical cutoff (nm)	Band gap (eV)
S-P-1	0	100	89	0.04	1.9	7.2±1	439.7	2.82
S-P-1a	20.6	79.4	/	/	/	6.4±0.5	/	/
S-P-2 (S-T-4)	68.5	31.5	141	0.05,0.04	4.5,15.2	7.5±0.5	417.5	2.97
S-P-3	88.1	11.9	135	0.05	2	5.8±0.5	405.2	3.06
S-P-4	100	0	159	0.06	3.9	6.7±1	392.4	3.16
S-T-1	/	/	156	0.05	1.4	/	/	/
S-T-2	100	0	95	0.03	0.5	10.5±0.5	/	/
S-T-3	91.8	8.2	103	0.03,0.02	1.8,9.3	6.8±0.5	/	/
S-T-5	42.3	57.7	135	0.04	5.6	6.0±1	/	/
S-T-6	0	100	131	0.04	3.6	6.9±0.5	/	/

Table S2. Ag content and the crystallite size in the Ag/TiO_2 composites

Samples	molar ratios of Ag (%)	Crystallite size (nm)
Ag/S-P-1	9.53	7.5±0.5
Ag/S-P-2/(Ag/S-T-4)	9.56	7.8±0.5
Ag/S-P-3	9.50	6.1±0.5
Ag/S-P-4	9.49	7.0±1
Ag/P25	9.51	20±1
Ag/S-T-1	9.49	/
Ag/S-T-2	9.51	11.0±0.5
Ag/S-T-3	9.53	7.0±0.5
Ag/S-T-5	9.52	6.1±1
Ag/S-T-6	9.54	7.2±1

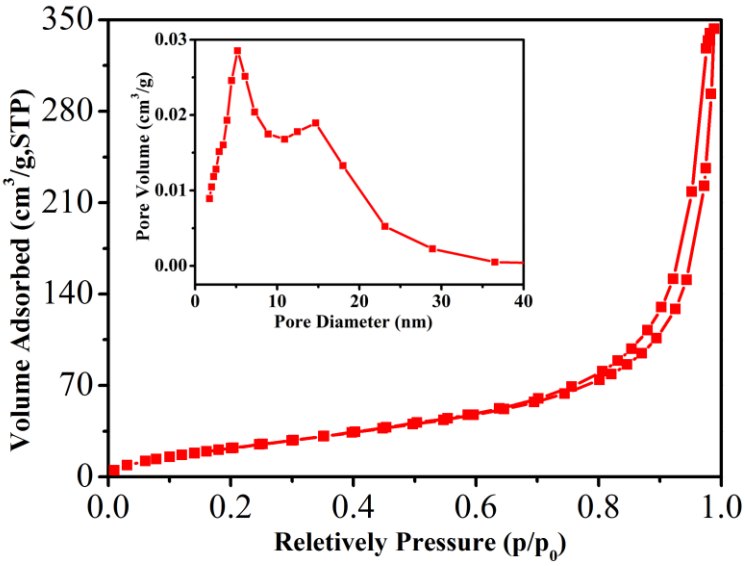

Fig. S1. N_2 adsorption–desorption isotherm curves and pore size distribution (inset) of S-T-4 sample.

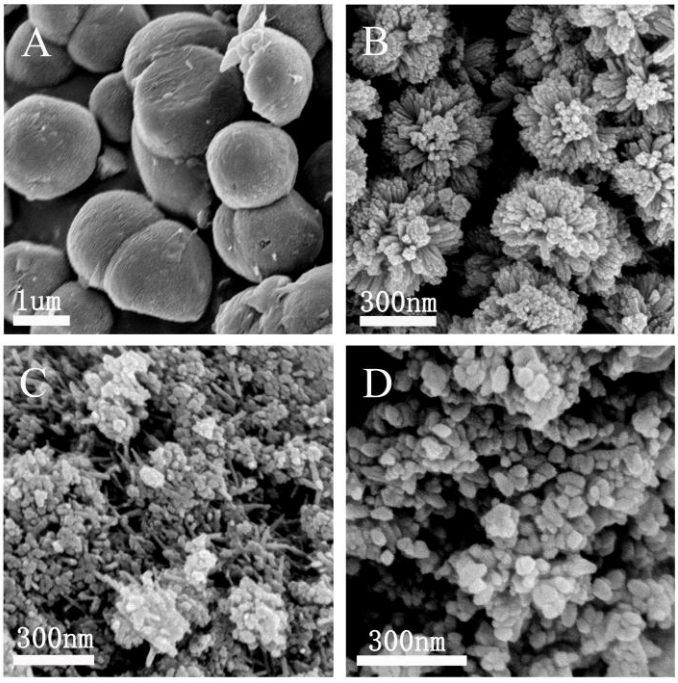

Fig. S2. SEM images of the products prepared from hydrothermal for 10 h at different pH values: (A) 0.35, (B) 0.97, (C) 2.10, (D) 3.15.

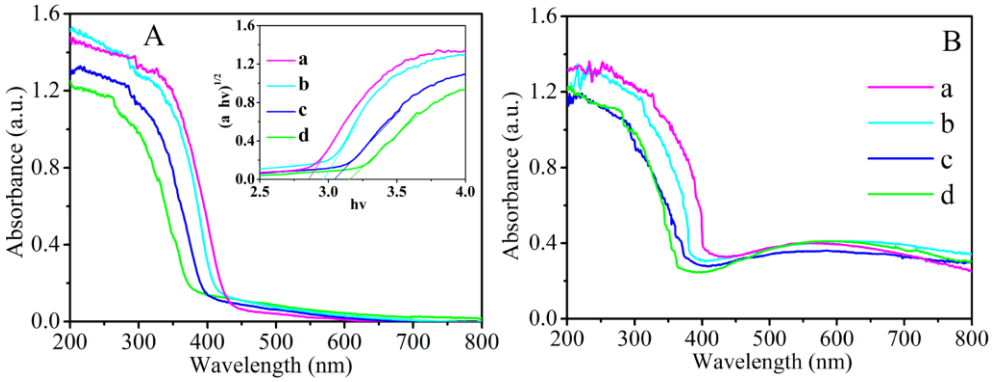

Fig. S3. UV−vis diffuse reflectance spectra (A) and plots of the corresponding $(\alpha h\upsilon)^{1/2}$ versus $(h\upsilon)$ (insert) of the as-synthesized materials prepared from different pH values: (a) S-P-1, (b) S-P-2, (c) S-P-3, (d) S-P-4; the corresponding UV−vis diffuse reflectance spectra (B) of Ag/TiO_2 samples: (a) Ag/S-P-1, (b) Ag/S-P-2, (c) Ag/S-P-3, (d) Ag/S-P-4.

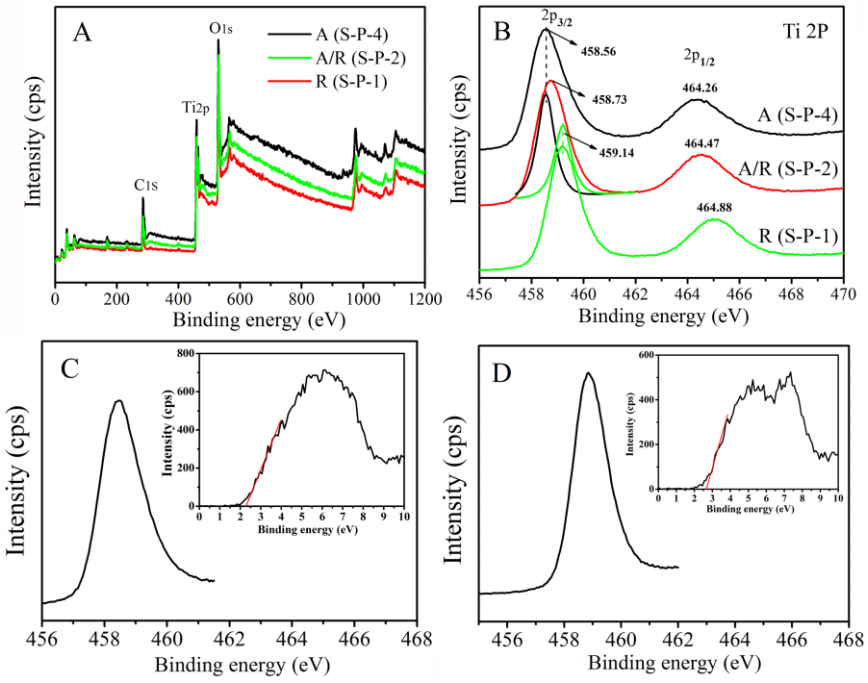

Fig. S4. XPS patterns of the prepared TiO_2 samples (A) XPS survey spectrum; (B) Ti_{2p} region of different samples; (C) Core level $Ti_{2p3/2}$ spectra and VB spectra for the bulk anantase sample (S-P-4); (D) Core level $Ti_{2p3/2}$ spectra and VB spectra for the bulk rutile sample (S-P-1).

Table S3 XPS Binding energies of the core levels and VBM of anatase, rutile, and anatase-rutile photocatalysts.

photocatalyst	state	binding energy (eV)
anatase (S-P-4)	$Ti_{2p3/2}$	458.56±0.05
	VBM	2.60±0.05
rutile (S-P-1)	$Ti_{2p3/2}$	459.14±0.05
	VBM	2.48±0.05
anatase-rutile (S-P-2)	$Ti_{2p3/2}$ (anatase)	458.56±0.05
	$Ti_{2p3/2}$ (rutile)	459.14±0.05

The energy difference of the $Ti_{2p3/2}$ (rutile) CL peak to VBM, $(E_{Ti2p}-E_{V.\ R})_{bulk}^{R}$, was determined to be 459.14 ± 0.05 eV, while that of anatase, $(E_{Ti2p}-E_{V.\ A})_{bulk}^{A}$, was 458.56 ± 0.05 eV.

The energy difference of anatase and rutile CLs, ΔE_{CL}, in the anatase-rutile heterostructure was evaluated to be 0.58 ± 0.05 eV. According to equation (1), the resulting VB offset (VBO), ΔE_V, was calculated to be 0.12 eV. Finally the CB offset (CBO) was estimated by the formula $\Delta E_C = \Delta E_V + E_g(\text{anatase}) - E_g(\text{rutile})$, where E_g(anatase) and E_g(rutile) are the optical band gap of anatase and rutile , respectively. Using the band gap of anatase (3.16 eV) and rutile (2.82 eV) determined by UV−visible diffuse reflectance spectroscopy (Table S1), the ΔE_C was calculated to be 0.22 ±0.05 eV that led to the proposed energy band diagram for the anatase-rutile sample shown in Fig. S5.

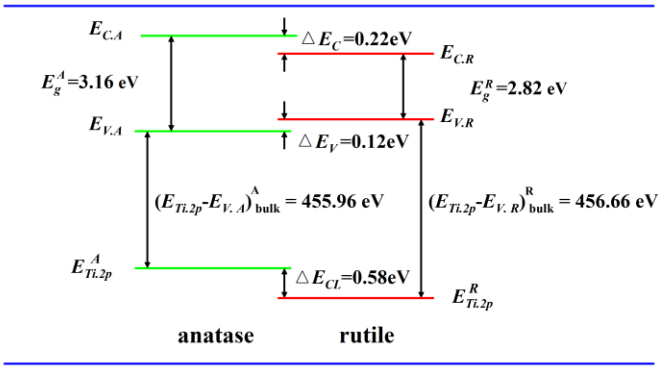

Fig. S5. Band alignment diagram of the anatase-rutile heterostructure (S-P-2).

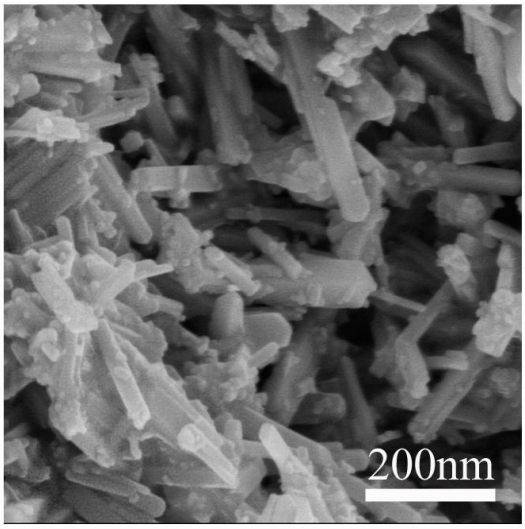

Fig. S6. SEM image of the TiO_2 sample prepared from hydrothermal reaction in the absence of PSS (10 h with pH=0.97).

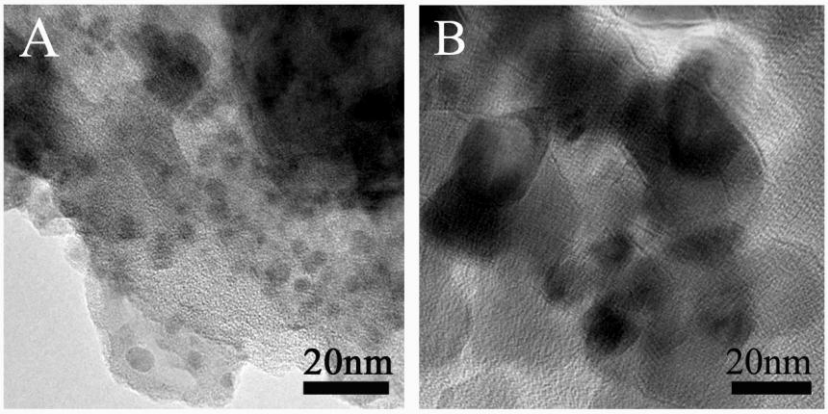

Fig. S7. TEM image of (A) Ag/hierarchical flower-like TiO_2 and (B) Ag/Degussa P25.

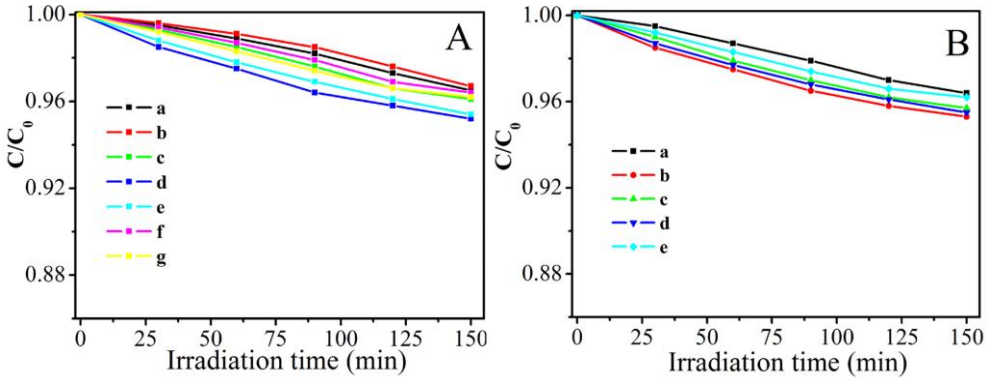

Fig. S8. Photocatalytic degradation of phenol under visible-light irradiation by different photocatalysts. A: (a) S-T-1, (b) S-T-2, (c) S-T-3, (d) S-T-4, (e) S-T-5 (f) S-T-6 and (g) Degussa P25. B: (a) S-P-1, (b) S-P-2, (c) S-P-3, (d) S-P-4 and (e) Degussa P25.

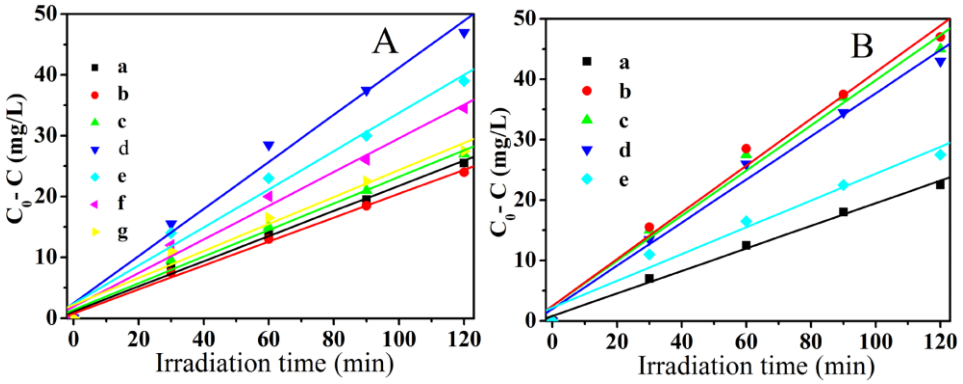

Fig. S9. Zero order kinetics of phenol degradation (50 mg/L) under UV light irradiation by different photocatalysts: A: (a) S-T-1, (b) S-T-2, (c) S-T-3, (d) S-T-4, (e) S-T-5 (f) S-T-6 and (g) Degussa P25. B: (a) S-P-1, (b) S-P-2, (c) S-P-3, (d) S-P-4 and (e) Degussa P25.

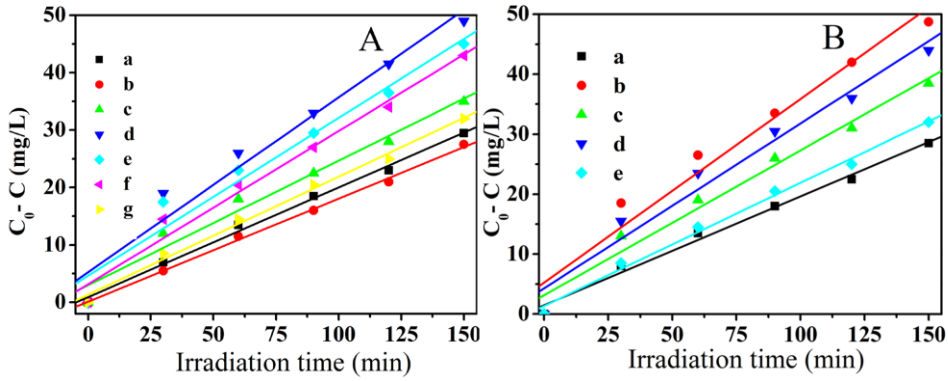

Fig. S10. Zero order kinetics of phenol degradation (50mg/L) under visible light irradiation by different photocatalysts: A: (a) Ag/S-T-1, (b) Ag/S-T-2, (c) Ag/S-T-3, (d) Ag/S-T-4, (e) Ag/S-T-5, (f) Ag/S-T-6, and (g) Ag/Degussa P25; B: (a) Ag/S-P-1, (b) Ag/S-P-2, (c) Ag/S-P-3, (d) Ag/S-P-4 and (e) Ag/Degussa P25.

Table S4. Apparent (k_r) and normalized (k_{norm}) rate constants for the degradation of phenol with the as-synthesized samples.

photocatalysts	k_r (g/L min)	k_{norm} (g^2/m^2 min L)	photocatalysts	k_r (g/L min)	k_{norm} (g^2/m^2 min L)
S-T-1	2.22×10^{-4}	1.42×10^{-6}	Ag/S-T-1	2.00×10^{-4}	1.28×10^{-6}
S-T-2	2.08×10^{-4}	2.19×10^{-6}	Ag/S-T-2	1.80×10^{-4}	1.89×10^{-6}
S-T-3	2.38×10^{-4}	2.31×10^{-6}	Ag/S-T-3	2.48×10^{-4}	2.41×10^{-6}
S-T-4 (S-P-2)	4.18×10^{-4}	2.96×10^{-6}	Ag/S-T-4 (Ag/S-P-2)	3.72×10^{-4}	2.64×10^{-6}
S-T-5	3.47×10^{-4}	2.57×10^{-6}	Ag/S-T-5	3.36×10^{-4}	2.38×10^{-6}
S-T-6	3.03×10^{-4}	2.31×10^{-6}	Ag/S-T-6	3.09×10^{-4}	2.36×10^{-6}
S-P-1	1.99×10^{-4}	2.24×10^{-6}	Ag/S-P-1	1.96×10^{-4}	2.20×10^{-6}
S-P-3	4.05×10^{-4}	3.00×10^{-6}	Ag/S-P-3	2.76×10^{-4}	2.04×10^{-6}
S-P-4	3.88×10^{-4}	2.44×10^{-6}	Ag/S-P-4	3.13×10^{-4}	1.96×10^{-6}
Degussa P25	2.52×10^{-4}	5.25×10^{-6}	Ag/DegussaP25	2.20×10^{-4}	4.58×10^{-6}

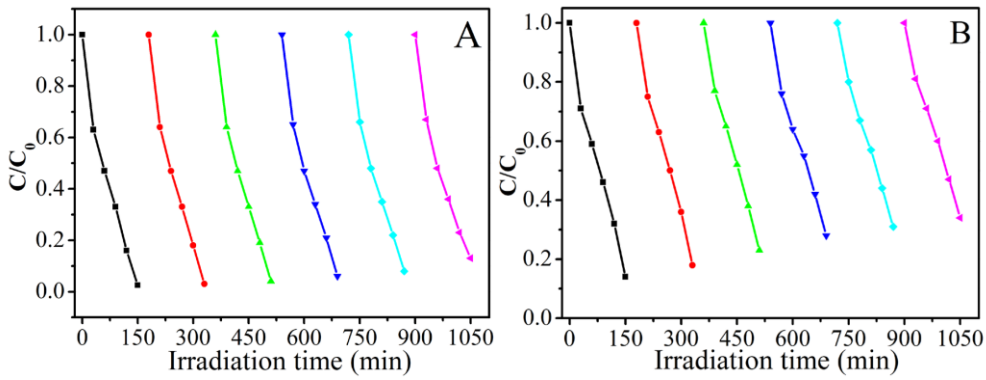

Fig. S11. Cycling runs in the photodegradation of phenol in the presence of (A) Ag/hierarchical flower-like TiO_2 and (B) Ag/Degussa P25 under visible light irradiation.

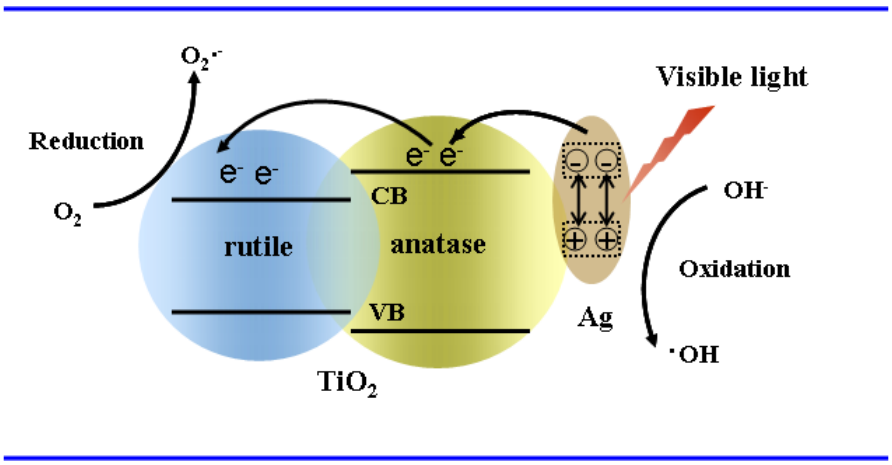

Fig. S12. Proposed mechanism for the photocatalytic degradation of phenol by the sample of Ag/S-T-4 nanocomposites under visible light irradiation.